Effects of laser irradiation on the morphology of Cu(110)

T. Brandstetter, M. Draxler, M. Hohage, and P. Zeppenfeld*
Institut für Experimentalphysik, Johannes Kepler Universität Linz, A-4040 Linz, Austria

T. Stehrer and J. Heitz
Institut für Angewandte Physik, Johannes Kepler Universität Linz, A-4040 Linz, Austria

N. Georgiev, D. Martinotti, and H.-J. Ernst†
CEA Saclay, DSM/Drecam/SPCSI, 91191 Gif sur Yvette, France
(Received 3 April 2008; published 18 July 2008)

The effects of pulsed laser irradiation on the morphology of the Cu(110) surface were investigated by means of reflectance difference spectroscopy (RDS) and spot profile analysis low-energy electron diffraction (SPA-LEED). The laser light induces surface defects (adatoms and islands) as well as subsurface dislocation lines. The high surface mobility leads to efficient annealing of the surface defects even at room temperature, whereas the subsurface dislocation lines persist up to temperatures $T>800$ K. SPA-LEED profiles of the (00) diffraction spot from the laser irradiated surface suggest an anisotropic distribution of the subsurface line defects related to the geometry of the fcc easy glide system, which is corroborated by STM measurements. Comparative experiments using conventional Ar ion bombardment point out the distinctiveness of the morphological changes induced by laser irradiation.

DOI: 10.1103/PhysRevB.78.035433 PACS number(s): 68.47.De, 61.80.Ba

I. INTRODUCTION

The understanding of the restructuring or patterning of surfaces during growth, erosion, or thermal treatment is of great relevance for the fabrication of surfaces and thin films with well defined physical or chemical properties. Whether the surface is rough, atomically flat, or regularly patterned at the micrometer or nanometer scale may strongly affect the mechanical and adhesion properties, the surface electronic structure, as well as its optical properties and catalytic activity. Single crystal surfaces under well defined conditions (usually in ultrahigh vacuum) have been studied experimentally by diffraction techniques and scanning probe microscopy (STM and AFM). Together with theoretical models and simulations, these studies have unraveled the driving forces and the atomic mechanisms governing the evolution of the surface morphology during deposition (growth), erosion (by low energy ion bombardment), or thermal treatment.[1,2]

As an example, the growth of Cu on flat and regularly stepped Cu surfaces leads to the formation of structural patterns at the nanometer scale.[3,4] Likewise, bombardment with low energy ions (typically Ar^+ with energies around 1 keV) removes impurities as well as substrate atoms (sputtering), which is exploited in standard surface cleaning procedures. In addition, ion bombardment has been successfully applied for the micro- and nanostructuring of both semiconductor and metal surfaces.[5] In this case, the pattern periodicity and dimensionality [i.e., the formation of one-dimensional (1D) vs two-dimensional (2D) structures] can be tuned by varying the experimental conditions such as ion-beam energy, flux, angle of incidence, and surface temperature.

Ion bombardment, however, also leads to the creation of subsurface defects and the implantation of the primary ions (Ar) as interstitial atoms and gas bubbles.[6] The presence of these subsurface defects deteriorates the crystalline quality of the sample and is often detrimental to the surface restructuring process. Other techniques such as laser irradiation as frequently used in material processing might provide an alternative, avoiding, in particular, ion implantation in the subsurface region. However, the interaction of high-power laser light with materials often causes irreversible damage in the near surface region, as the optical energy of the laser pulses is dissipated in a transient temperature rise that produces temperature-induced melting or thermomechanical strain leading to plastic deformation. On the other hand, for moderate intensities as applied in our experiments, no structural modification should occur at all. Indeed, the maximum transient temperature rise for bulk copper assuming a Gaussian beam with a few millimeters diameter, wavelength 532 nm, 6 ns pulse length, and an intensity of 20 MW/cm^2 can be estimated to be about 200 K in the beam center.[7] The expected maximum temperatures are thus far below the melting point of Cu at 1357 K. The threshold of laser ablation has been reported to be at 300 mJ/cm^2 (50 MW/cm^2) for copper under similar conditions, which is considerably higher than the intensities used here.[8]

It thus came as a surprise when Ernst *et al.*[9] could demonstrate that Cu(100) and Cu(111) single-crystal surfaces can, indeed, be patterned by laser light at such small incident laser intensities. Helium atom beam scattering (HAS) and scanning tunneling microscopy (STM) experiments revealed that irradiation with green laser light at a moderate fluence of 114 mJ/cm^2 per 10 ns pulse produces adatoms, which self-organize into nanoscale pyramids, similar to those found in the growth of Cu on Cu surfaces.[4] In contrast to green light, infrared (IR) laser irradiation at an equivalent absorbed energy density does not produce any structural change. This, for metallic systems unforeseen, spectral difference in laser action implies that the primary electronic excitation must play a key role in the surface restructuring. Yet, the precise nature of the primary excitation (long-lived excitonlike state originating from the excitation of Cu 3*d* electrons or local-

ized surface plasmons) as well as the mechanism leading to the subsequent generation of surface adatoms and defects is still unclear.

Besides the adatom and vacancy islands created upon laser irradiation, later STM studies performed on the Cu(100) surface at lower surface temperatures[10] further revealed an oriented network of step edges which is most likely related to edge dislocations along the fcc easy glide system. In fact, this network is actually responsible for the alignment of the pyramids apparent in Fig. 2 of Ref. 9. Whereas, the more prominent surface pattern can be completely removed by annealing for a couple of minutes at 560 K;[9] we presume that if edge dislocations are created during laser irradiation, the associated subsurface line defects should persist up to much higher annealing temperatures.

In the present study, a Cu(110) surface was chosen for further investigation of the morphological changes induced by laser irradiation with particular emphasis on the possible formation of subsurface defects such as dislocation lines. The Cu(110) surface is anisotropic as would be the orientation of an edge dislocation network associated with the fcc easy glide system. In addition to well established surface analytical techniques, namely spot profile analysis low-energy electron diffraction (SPA-LEED) and STM, we have applied reflectance difference spectroscopy (RDS), which turns out to be a powerful tool for the *in situ* and real-time characterization of surface defects as well as subsurface dislocation lines induced by laser irradiation.

II. EXPERIMENT

The experiments were performed in a UHV chamber with a base pressure below 10^{-10} mbar. The chamber is equipped with an Auger-electron spectrometer (AES) to check the sample cleanliness, a quadrupole mass analyzer (QMA), and a SPA-LEED system. The high quality Cu(110) sample can be cooled by liquid nitrogen via a Cu braid and heated by electron bombardment from the backside. The sample surface is prepared *in situ* by 900 eV Ar^+ bombardment and subsequent annealing at 900 K for 5 min. An RD spectrometer can be attached to the chamber and the light is coupled in via a strain free optical window. RDS measures the normalized difference in reflectivity at normal incidence for light polarized along two mutually perpendicular orientations (x,y) of the polarization vector as a function of photon energy:[11,12]

$$\frac{\Delta r}{r} = 2\frac{r_x - r_y}{r_x + r_y}. \tag{1}$$

For cubic crystals, the response from the optically isotropic bulk cancels by symmetry and the signal is exclusively due to the in-plane optical anisotropy within the surface region. The sample can be irradiated with laser light that is coupled into and out of the chamber through two quartz windows. The laser beam hits the sample under an angle of about 10° with respect to the surface normal. The sample, laser windows, and RDS window are aligned in a way that allows the measurement of the RDS response of the sample during laser irradiation. Also, the sputtering of the crystal by Ar^+ bombardment takes place at the same sample position and can therefore be monitored by RDS. As a light source, a Nd:YAG laser (Continuum, Surelite I-20) and a frequency doubling crystal (KDP, potassium dihydrogen phosphate) was used, generating light pulses with a temporal width of 6 ns at a wavelength of $\lambda = 532$ nm. By means of a diffuser plate and a collimating lens, a nearly Gaussian beam profile was obtained, which however showed a distinct speckle pattern. The beam profile was analyzed and fitted by a beam profiler (Laser 2000, WinCam D) with a variable attenuator. Applying a $1/e^2$ criterion, the effective beam diameter was 3.1 mm, which is slightly smaller than the estimated diameter of the RDS spot of about 4 mm. Therefore, the RD signals from the laser irradiated surface always contain a fraction of the signal from the nonirradiated surface. The laser-pulse energy was measured by a pyroelectric detector (Ophir, PE50-SH-V2).

III. RESULTS AND DISCUSSION

Figure 1(a) shows a comparison of RD spectra recorded at 210 K from a clean Cu(110) surface before (squares) and after (circles) irradiation with 500 pulses of green (532 nm) laser light with an effective incident fluence of 134 mJ/cm^2 and a repetition rate of 1 Hz. Figure 1(a) reveals two different types of changes in the optical anisotropy of the surface. One is due to the quenching of surface states related transitions and appears as a reduction of the positive peak at 2.1 eV and of the small negative peak at 3.9 eV. These features involve anisotropic transitions from an occupied surface state to an empty surface state at the $\bar{Y}$ point and from an occupied surface resonance to an empty surface state at $\bar{X}$, respectively.[13,14] The other one appears as a change of the negative peak at 4.3 eV, a feature that is attributed to a surface modified bulk transition at the L symmetry point of the bulk Brillouin zone.[13,15] It is known that the intensity at 4.3 eV strongly depends on the surface strain field and is modified by higher order terms of the spatial strain distribution even if the average strain (bending) of the surface is zero.[16]

In similar experiments on the Cu(100) surface performed by Ernst *et al.*,[9] STM revealed that laser irradiation induces adatom and vacancy islands as well as edge dislocations along the fcc easy glide system.[10] According to this, the quenching of the surface state related features at 2.1 and 3.9 eV can be attributed to scattering and quenching of the surface states by surface defects and by step edges formed at the surface as a consequence of the formation of subsurface dislocation lines. The bulk related feature at 4.3 eV, on the other hand, is more likely to be sensitive to the near surface strain field caused by the dislocations. In the following, we will concentrate on the RD signals at 2.1 and 4.3 eV in order to monitor in a complementary way the formation and annealing of surface defects and subsurface dislocations, respectively.

In Fig. 1(b), the evolution of the RD spectrum during laser irradiation is plotted as a function of time at fixed photon energies of 2.1 and 4.3 eV. It shows that the change of the 4.3 eV feature (circles) saturates after approximately 50 laser pulses (50 s). This does not necessarily mean that from

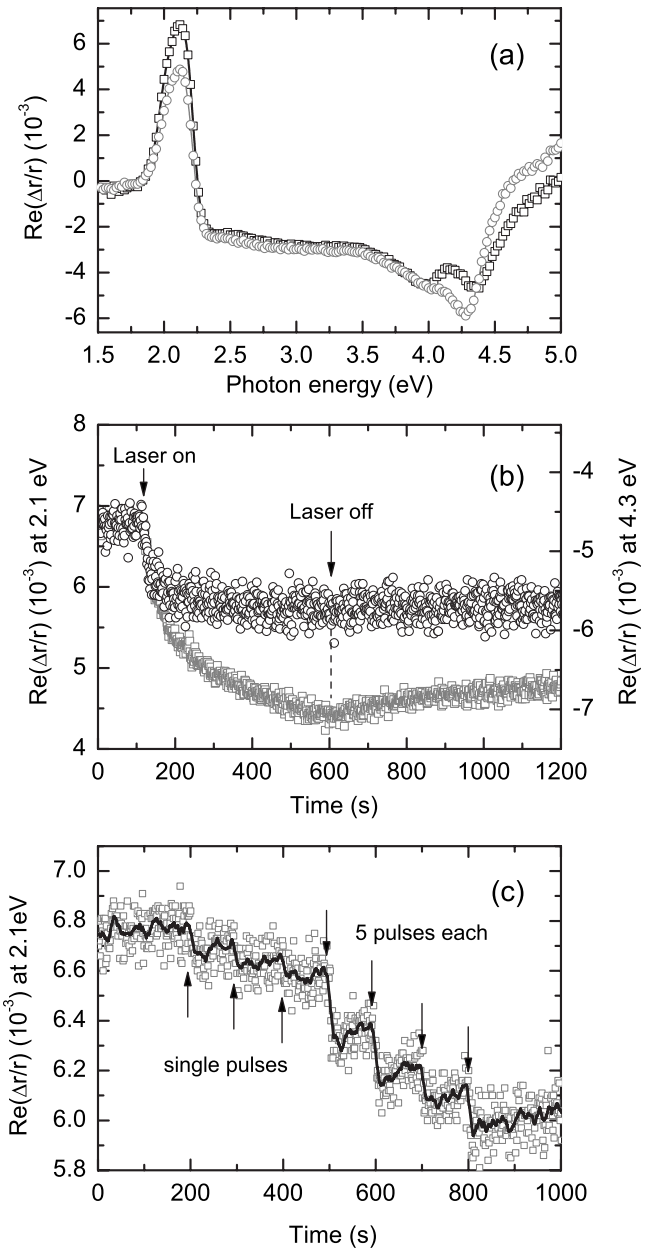

FIG. 1. (a) RD spectrum of Cu(110) before (squares) and after irradiation (circles) with 500 pulses of green laser light at an incident fluence of 134 mJ/cm^2 at 210 K. (b) Evolution of the RD spectrum during laser irradiation plotted as a function of time for fixed photon energies of 2.1 eV (squares) and 4.3 eV (circles). The pulse repetition rate was 1 Hz. (c) RDS intensity at 2.1 eV plotted as a function of time during laser irradiation with an incident fluence of 134 mJ/cm^2 at 210 K. The solid line corresponds to a ten point adjacent averaging of the data.

this point on, no further dislocations are created. As already mentioned, the RD signal at this energy is sensitive to the changes in the spatial strain distribution.[16] Therefore, the saturation of the RD signal at 4.3 eV could just mark the point where the dislocation lines have reached a critical density at which their individual strain fields start to overlap.

Another point that can be seen from Fig. 1(b) is that the intensity at 2.1 eV (squares) starts to recover as soon as the laser is turned off. According to our interpretation, the reduction of this feature during laser irradiation is related to the creation of defects on the surface. This would mean that the mobility at the static sample temperature of 210 K, at which the experiment was carried out, is high enough for these defects to anneal at a detectable rate. A similar result is obtained if the irradiation is interrupted after a few laser pulses, as depicted in Fig. 1(c). Again, surface defects are created during each series of pulses, giving rise to the steplike decrease of the RD signal at 2.1 eV. Between successive bursts, however, the surface defects are partially healed as indicated by the slow increase of the RD signal. In the experiment presented in Fig. 1(c) the polarization direction of the laser light coincided with the crystallographic $[\bar{1}10]$ direction of Cu(110), one of the two main symmetry directions of this surface. Experiments performed under the same conditions but with the orthogonal polarization direction of the laser light yielded results that were indistinguishable within experimental error from those presented in Fig. 1(c). Therefore, no influence of the polarization direction could be detected.

Figure 1(c) also demonstrates that the effect of a single laser pulse is detectable with RDS at 210 K. However, if the experiment is carried out at room temperature at the same laser fluence, the RD signal at 2.1 eV does not change at all. This can be explained by a higher surface mobility at room temperature as compared to 210 K, which allows the laser induced surface defects to heal at a rate beyond the time resolution of the RDS. Contrary to the RD feature at 2.1 eV, the RD signal at 4.3 eV in Fig. 1(b) does not change when the laser is turned off. Moreover, it is not affected by annealing up to a temperature of 500 K.

To point out the distinctiveness of the morphological changes induced by laser irradiation, similar measurements were performed on a Cu(110) surface after conventional 900 eV Ar^+ bombardment at 210 K for 25 min. Figure 2(a) shows a comparison of RD spectra recorded from the clean Cu(110) surface before (squares) and after (circles) Ar^+ bombardment. Contrary to the laser irradiation experiment presented in Fig. 1(a), the Ar^+ bombardment almost completely destroys the surface state related feature at 2.1 eV, indicating a stronger roughening of the surface. The change in the high energy part of the spectrum induced by Ar^+ bombardment is attributed to strain induced by subsurface point defects such as vacancies and argon bubbles[6] rather than to dislocation lines as in the case of laser irradiation. This gives rise to the different kinds of alterations in the spectra presented in Figs. 2(a) and 1(a), respectively. The evolution of the RD spectrum during Ar^+ bombardment monitored at a fixed photon energy of 2.1 eV and plotted as a function of time [Fig. 2(b)] shows that the surface state is destroyed almost completely in the very first phase of the bombardment and slightly recovers as soon as it is stopped. As for the case of laser irradiation, this recovery is interpreted as a partial annealing of the induced surface defects.

In Fig. 3(a), the influence of annealing after laser irradiation is displayed for the two main RDS features. The Cu(110) surface was irradiated with 500 pulses of green laser light with an incident fluence of 134 mJ/cm^2 at a static temperature of 210 K and then annealed at increasing tempera-

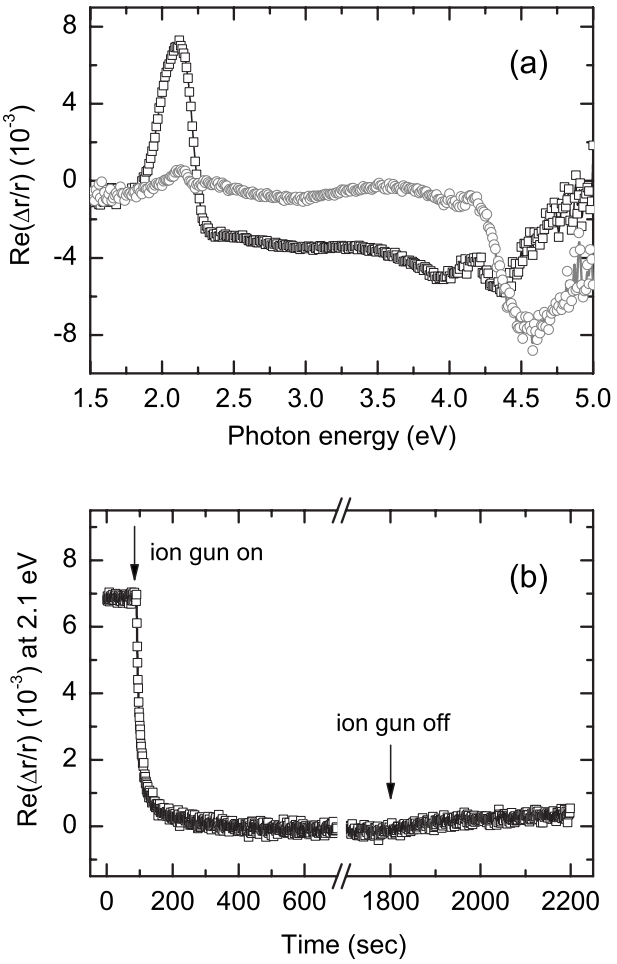

FIG. 2. (a) RD spectrum of Cu(110) before (squares) and after Ar^+ bombardment (circles) at 210 K. (b) Evolution of the RD spectrum during Ar^+ bombardment plotted as a function of time for a fixed photon energy of 2.1 eV.

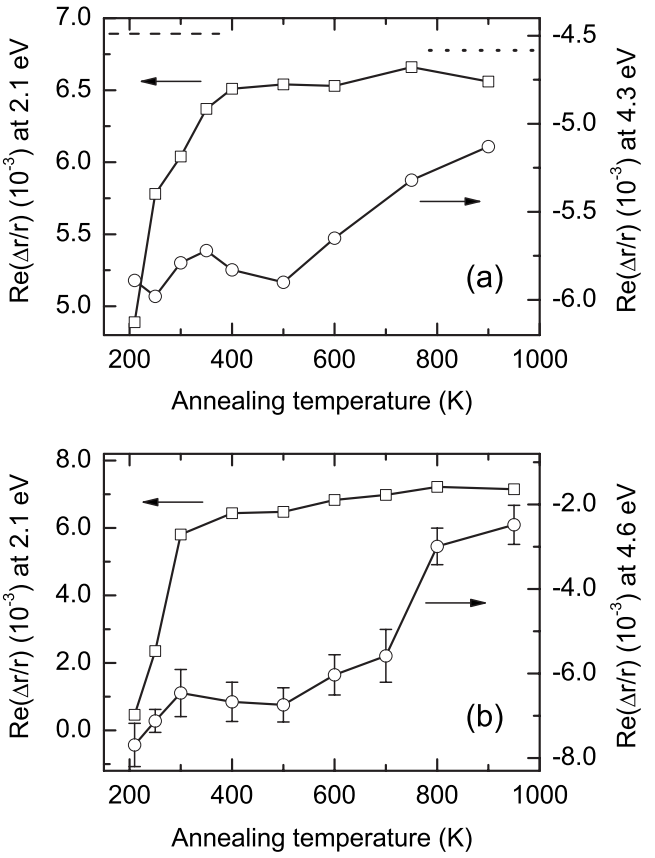

FIG. 3. (a) Intensities of the RD signals at 2.1 eV (squares) and 4.3 eV (circles) as a function of annealing temperature after irradiation with 500 pulses of green laser light at an incident fluence of 134 mJ/cm^2 at 210 K. RDS intensities of the nonirradiated surface are represented by the dashed and dotted lines for 2.1 and 4.3 eV, respectively. (b) Intensities of the RD signal at 2.1 eV (squares) and 4.6 eV (circles) as a function of annealing temperature after 900 eV Ar^+ bombardment at 210 K.

tures. The RDS intensities plotted in Fig. 3(a) were recorded after each annealing cycle when the sample was cooled down to 210 K again. The dashed and dotted lines represent the intensities measured before laser irradiation at 2.1 and 4.3 eV, respectively. Again, the different origins of the two RDS features are obvious. While the rapid increase of the surface-atom mobility around 250 K immediately leads to a flattening of the surface and, hence, to a recovery of the surface state related RD signal at 2.1 eV, the dislocations themselves (represented by the RDS intensity at 4.3 eV) are much more persistent. Even after annealing at 900 K, the surface is not restored completely.

For comparison, the influence of annealing on the RDS signals after Ar^+ bombardment is presented in Fig. 3(b). It shows a quite similar behavior for the RDS signals at 2.1 eV and in the strain related high energy range (here the position of the new minimum at 4.6 eV in the spectrum after Ar^+ bombardment was chosen). The 2.1 eV signal is almost fully recovered at 400 K in both cases indicating that the surface mobility at this temperature is high enough to locally flatten the surface. Despite their different origins, also the high energy features related to the Ar^+ bombarded and the laser irradiated surface, respectively, show a similar behavior upon annealing as far as the onset at about 500 K is concerned. However, contrary to annealing after laser irradiation, the signals from the ion bombarded surface are fully recovered after annealing at 950 K, which is self-evident, since the sample was originally prepared by means of Ar^+ sputtering and annealing.

The morphological changes induced by laser irradiation of the Cu(110) surface can also be observed with SPA-LEED. As an example, Fig. 4 displays profiles of the (00) diffraction spot along the [001] direction ($\bar{\Gamma}\bar{Y}$) using a primary beam energy $E=358$ eV which corresponds to 'in-phase' scattering condition for terraces with integer step height.[17] The profiles were taken before (black dashed) and after laser irradiation (gray solid), after annealing at 1000 K for 10 min (black solid), and after additional Ar^+ sputtering and subsequent annealing at 900 K (gray dashed). The data clearly show that an annealing temperature of 1000 K is not enough to completely recover the initial, narrow spot profile. At this high temperature, adatom or vacancy islands as well as any surface steps with integer height, induced by edge dislocations whose Burgers vector matches a lattice vector, should be fully annealed by surface-atom diffusion. How-

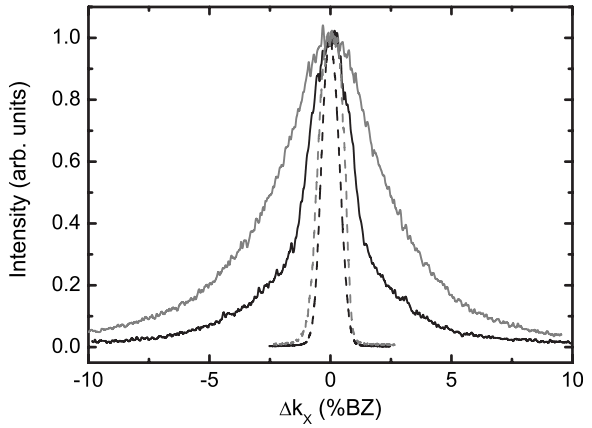

FIG. 4. SPA-LEED profiles of the (00) diffraction spot along the [001] direction (electron-beam energy $E=358$ eV) taken before (black dashed) and after laser irradiations (gray solid), after annealing at 1000 K for 10 min (black solid), and after additional Ar^+ sputtering and subsequent annealing at 900 K (gray dashed).

ever, the atomic displacements associated with the strain fields of the subsurface dislocation lines are still present and detectable with SPA-LEED. Possibly, other types of dislocations, characterized by Burgers vectors that are not integer multiples of a lattice vector, could cause stacking faults with noninteger height step edges on the surface. Such step edges cannot be simply annealed by detachment and lateral diffusion of surface atoms and might also contribute to the considerable broadening of the diffraction spot profiles even after the sample has been annealed at elevated temperatures.

Further details on the surface morphology and the annealing process can be obtained from SPA-LEED profiles by evaluating the full widths at half maximum ΔQ of the elliptical (00) diffraction spot as shown in Fig. 5(a). Here, ΔQ was measured for the two symmetry directions $[\bar{1}10]$ (circles) and [001] (squares) of the Cu(110) surface and plotted as a function of annealing temperature after the surface was irradiated with 120 pulses of green laser light at an incident fluence of 134 mJ/cm^2 at 210 K. Similar to the behavior of the 4.3 eV RDS feature, the SPA-LEED profiles recorded under in-phase condition appear to be mostly sensitive to those defects and local strain fields that are directly related to the presence of the dislocations, since ΔQ only starts to recover above 500 K along both directions.

In contrast to the annealing after laser irradiation, Fig. 5(b) shows the evolution of ΔQ along the $[\bar{1}10]$ direction upon annealing after Ar^+ bombardment of the pristine surface. Obviously, the behavior is quite different from what is observed after laser irradiation [Fig. 5(a)]. First, ΔQ starts at a much higher value indicating an initially much lower order at the surface right after ion bombardment. Second, it shows a steep decrease between 200 and 300 K which coincides with the recovery of the 2.1 eV RDS signal in Fig. 3(b) and is attributed to the annealing of surface defects. Third, another decrease of ΔQ sets in at 500 K. It is ascribed to the annealing of subsurface point defects. This process appears to be completed at around 700 K where ΔQ reaches its minimum. However, according to Fig. 3(b), the 4.6 eV RDS signal is not fully recovered below 800 K. This suggests that

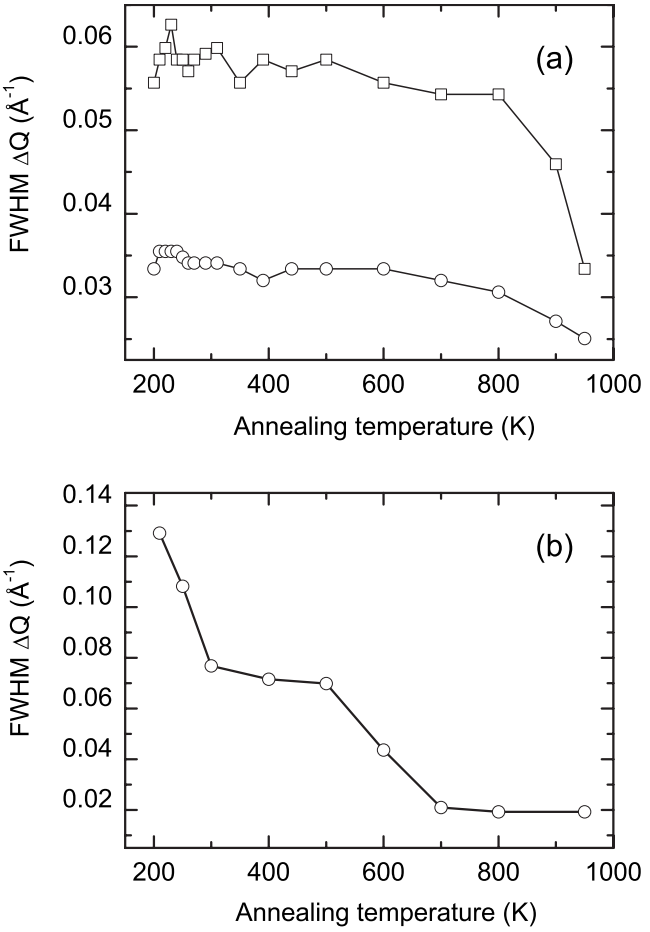

FIG. 5. (a) Full widths at half maximum ΔQ of the LEED (00) diffraction spot (electron-beam energy $E=358$ eV) for the two symmetry directions $[\bar{1}10]$ (circles) and [001] (squares) of the Cu(110) surface as a function of annealing temperature. Initially, the surface was irradiated at 210 K with 120 pulses of green laser light at an incident fluence of 134 mJ/cm^2. (b) Full widths at half maximum ΔQ of the SPA-LEED (00) diffraction spot along the $[\bar{1}10]$ direction of the Cu(110) surface as a function of annealing temperature. Initially the surface was bombarded with 900 eV Ar^+ ions at 210 K.

RDS is actually more sensitive to this kind of subsurface defects.

The different values of ΔQ for the two symmetry directions after laser irradiation can be understood by the asymmetry of the fcc easy glide system projected onto the (110) surface. To this end, the measured ΔQ are first corrected for instrumental broadening (which is almost negligible in the present case) and then converted to a characteristic length scale $D=2\pi/\Delta Q$ and a corresponding linear density $\rho=1/D$ which can be interpreted as the average spacing and density, respectively, of line defects such as step edges and dislocation lines. Subtracting the defect density ρ_0 obtained for the nonirradiated surface, one can thus estimate the density $\tilde{\rho}=\rho-\rho_0$ or spacing $\tilde{D}=1/\tilde{\rho}$ of the line defects created during laser irradiation. Assuming that during irradiation and for temperatures below the onset of annealing, the probability to create a dislocation line is the same for each of the four

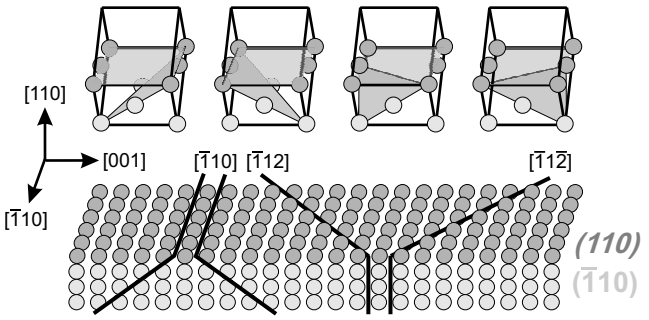

FIG. 6. Projection of the fcc easy glide system onto the (110) surface.

{111} oriented slip planes, the step edges formed on the (110) surface are parallel to the [$\bar{1}$10], the [$\bar{1}$12], and the [$\bar{1}1\bar{2}$] directions in the relative proportion of 2:1:1 (see Fig. 6). It is then straightforward to determine the ratio of the average linear density or spacing between subsequent step edges along the [$\bar{1}$10] and [001] directions, respectively:

$$\frac{\tilde{D}_{[\bar{1}10]}}{\tilde{D}_{[001]}} = \frac{\cos\alpha + 1}{\sin\alpha} = \frac{\sqrt{3}+1}{\sqrt{2}} \approx 1.93. \tag{2}$$

Here, $\alpha = \arctan\sqrt{2} \approx 54.74°$ is the inclination of the [$\bar{1}$12] and [$\bar{1}1\bar{2}$] oriented step edges with respect to the [$\bar{1}$10] direction. The calculated value is in excellent agreement with the ratio of 1.92 extracted from the data in Fig. 5(a). The fact that this anisotropy persists up to annealing temperatures of 800 K, underlines the assumption that SPA-LEED measurements close to in-phase scattering conditions are mainly sensitive to the laser induced, subsurface dislocation lines.

To confirm our interpretation and the presence of [$\bar{1}$10] and [$\bar{1}$12] oriented dislocation lines, Fig. 7 shows an STM image of a Cu(110) surface after irradiation with 20 pulses of green (532 nm) laser light with a temporal width of 10 ns and an effective incident fluence of 90 mJ/cm^2 at 200 K. It was recorded in a different experimental setup and since the irradiation parameters do not exactly match those of the RDS and SPA-LEED experiments, the results cannot be compared quantitatively. Nevertheless, the STM image reveals two dislocation lines identified by the two extended (monatomic) step edges running straight across the surface. The associated dislocation lines are, indeed, oriented along the [$\bar{1}$10] and [$\bar{1}$12] directions, respectively, and thus support our explanation of the anisotropic broadening of the SPA-LEED (00) diffraction spot and the change in the 4.3 eV RDS feature. In addition, Fig. 7 shows islands of monatomic height that could be responsible for the reduction of the surface states

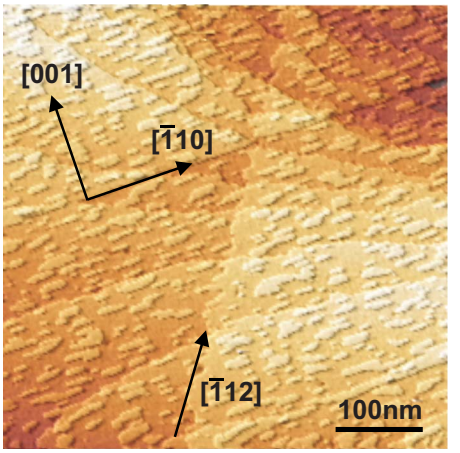

FIG. 7. (Color online) STM image (500×500 nm^2) of the Cu(110) surface after irradiation with 20 pulses of green laser light at an incident fluence of 90 mJ/cm^2 at 200 K.

related RD signal at 2.1 eV. Contrary to the measurements after Ar^+ bombardment, where the initial roughness of the surface was high enough to completely destroy the 2.1 eV RDS feature, SPA-LEED close to in-phase scattering conditions does not seem to be sensitive to the more moderate changes in surface morphology induced by laser irradiation. In particular, there is no detectable change in ΔQ in Fig. 5(a) during the recovery of the surface states related RD signal between 200 and 400 K as observed in Fig. 3(a).

IV. SUMMARY

We have shown that irradiation of a Cu(110) surface with green laser light induces surface defects and subsurface dislocation lines. Both types of defects lead to distinct and spectrally separated changes in the RD spectrum. The formation of these defects during irradiation as well as their behavior upon thermal annealing was characterized. The morphological changes induced by laser irradiation were compared to those induced by bombardment with 900 eV Ar^+ ions. The anisotropic defect density obtained on the laser irradiated surface was explained by the geometry of the fcc easy glide system assuming that the dislocations are created along the {111} oriented slip planes. This assumption is supported by STM measurements.

ACKNOWLEDGMENTS

This work was financially supported by the Austrian Academic Exchange Service (ÖAD) through AMADEE Project No. 16/2006, the Austrian Science Fund (FWF) through Projects No. P17360 and No. S9002, and by PAI Amadeus Project No. 10641XD. The authors also want to thank D. Bäuerle for helpful discussions and T. Maroutian and F. Merlet for their support during the STM experiments at Saclay.

*peter.zeppenfeld@jku.at
†Dr. Ernst died on April 29, 2008.

[1] T. Michely and J. Krug, *Islands, Mounds, and Atoms: Patterns and Processes in Crystal Growth Far from Equilibrium*, Springer Series in Surface Sciences Vol. 42 (Springer, Heidelberg, 2004).
[2] H. Brune, Surf. Sci. Rep. **31**, 125 (1998).
[3] H.-J. Ernst, F. Fabre, R. Folkerts, and J. Lapujoulade, Phys. Rev. Lett. **72**, 112 (1994).
[4] N. Néel, T. Maroutian, L. Douillard, and H.-J. Ernst, Phys. Rev. Lett. **91**, 226103 (2003).
[5] U. Valbusa, C. Boragno, and F. Buatier de Mongeot, J. Phys.: Condens. Matter **14**, 8153 (2002).
[6] M. Hohage, L. D. Sun, and P. Zeppenfeld (unpublished).
[7] D. Bäuerle, *Laser Processing and Chemistry*, 3rd ed. (Springer-Verlag, Berlin, 2000).
[8] R. Jordan, D. Cole, J. G. Lunney, K. Mackay, and D. Givord, Appl. Surf. Sci. **86**, 24 (1995).
[9] H.-J. Ernst, F. Charra, and L. Douillard, Science **279**, 679 (1998).
[10] H.-J. Ernst, F. Charra, and L. Douillard (unpublished).
[11] D. E. Aspnes, J. P. Harbison, A. A. Studna, and L. T. Florez, J. Vac. Sci. Technol. A **6**, 1327 (1988).
[12] D. S. Martin and P. Weightman, Surf. Interface Anal. **31**, 915 (2001).
[13] K. Stahrenberg, Th. Herrmann, N. Esser, and W. Richter, Phys. Rev. B **61**, 3043 (2000).
[14] L. D. Sun, M. Hohage, P. Zeppenfeld, and R. E. Balderas-Navarro, Surf. Sci. **589**, 153 (2005).
[15] L. D. Sun, M. Hohage, P. Zeppenfeld, R. E. Balderas-Navarro, and K. Hingerl, Surf. Sci. **527**, L184 (2003).
[16] L. D. Sun, M. Hohage, P. Zeppenfeld, R. E. Balderas-Navarro, and K. Hingerl, Phys. Rev. Lett. **96**, 016105 (2006).
[17] M. Horn-von Hoegen, Z. Kristallogr. **214**, 1 (1999).